The Annals of Applied Probability
2001, Vol. 11, No. 4, 1137–1165

STOCHASTIC PARTICLE APPROXIMATIONS FOR SMOLUCHOSKI'S COAGULATION EQUATION[1]

BY ANDREAS EIBECK AND WOLFGANG WAGNER

Weierstrass Institute for Applied Analysis and Stochastics

This paper studies stochastic particle approximations for Smoluchowski's coagulation equation. A new stochastic algorithm with reduced variance is proposed. Its convergence behavior is investigated, when the number of simulation particles tends to infinity. Under appropriate assumptions on the coagulation kernel, the limit is the unique solution of the coagulation equation. Then detailed numerical experiments are performed, testing the applicability and efficiency of the algorithm. In particular, the gelation phenomenon (loss of mass in the coagulation equation) is studied numerically for several kernels. A striking feature of the new algorithm is a better convergence after the gelation point, providing a tool for detecting the mass of the gel.

1. Introduction. Smoluchowski's coagulation equation [32]

$$\begin{aligned}\frac{\partial}{\partial t}\,c(t,x) &= \tfrac{1}{2}\sum_{y=1}^{x-1} K(x-y,\,y)\,c(t,x-y)\,c(t,y)\\ &\quad -\sum_{y=1}^{\infty} K(x,\,y)\,c(t,x)\,c(t,y),\end{aligned}\tag{1.1}$$

where $t \geq 0$ and $x = 1, 2, \ldots,$ describes the time evolution of the average concentration of particles of a given size in some physical system. Concentration of particles of size x increases as a result of coagulation of particles of sizes $x - y$ and y. It decreases if particles of size x merge with any other particles. The intensity of the process is governed by the coagulation kernel K. The phenomenon of coagulation occurs in a wide range of applications, for example, in astrophysics, biology, chemistry and meteorology (see the survey papers [8] and [2]).

Stochastic particle systems play an important role in the study and numerical treatment of equation (1.1) and its continuous analogon

$$\begin{aligned}\frac{\partial}{\partial t}c(t,x) &= \tfrac{1}{2}\int_0^x K(x-y,\,y)c(t,x-y)\,c(t,y)\,dy\\ &\quad -\int_0^{\infty} K(x,\,y)c(t,x)c(t,y)\,dy,\end{aligned}\tag{1.2}$$

Received May 2000; revised October 2000.
[1]Supported by Deutsche Forschungsgemeinschaft.
AMS 2000 *subject classifications*. Primary 60K40, 65C35.
Key words and phrases. Stochastic particle method, coagulation equation, variance reduction, gelation phenomena.

where $x \in (0, \infty)$. The standard stochastic model related to the coagulation equation is a Markov jump process where two different clusters of size x and y coagulate to a single cluster of size $x + y$ with rate $K(x, y)$. This model is called Marcus-Lushnikov process (cf. [26], [25]). Qualitative properties of the coagulation equation and its generalizations have been studied using the stochastic approach, for example, in [20], [16], [27], [10]. For more details on the relationship between stochastic particle systems and the coagulation equation we refer to the excellent review [2].

When dealing with a numerical algorithm, the basic problem is to study its approximation properties. In case of stochastic algorithms for nonlinear equations, there are two main sources of error. First there is the systematic error representing the deviation of the expectation from the correct value, which is achieved when the number of particles goes to infinity. As in the deterministic case, the convergence rate for this type of error is of considerable interest with respect to the practical applicability of an algorithm. Second there is the statistical error due to the fluctuations of the generated sample of the process around its expected value. The presence of this type of error leads to a specific problem in the case of stochastic numerical algorithms, namely the problem of variance reduction - to construct stochastic processes having similar convergence properties with respect to the systematic error, but smaller fluctuations when estimating concrete functionals. This is a challenging problem in connection with stochastic algorithms for nonlinear equations (cf., e.g., [12], Chapter 4 concerning standard Monte Carlo theory).

Many stochastic algorithms for the coagulation equations (1.1), (1.2) are based on the classical Marcus-Lushnikov process (cf. [14], [15], [7], [31], [13], [18], [9]). These algorithms provide solutions in the limit of the number of particles going to infinity. Corresponding convergence properties, under appropriate assumptions on the coagulation kernel, can be derived from results in [17], [20], [27], [10]. Various numerical methods for the coagulation equation are reviewed in [30], where also an extended list of references is given. Some stochastic algorithms contain an additional approximation parameter (time step), thus providing solutions to time discretized versions of the coagulation equations (1.1), (1.2) (cf. [24], [22], [29], [28], [21]). An approach to the variance reduction problem within this class of algorithms is presented in [3]. Some ideas of that approach will be used in the present paper.

The *purpose of this paper* is to propose a new stochastic algorithm for the numerical treatment of the coagulation equations (1.1), (1.2) and to investigate its systematic and statistical error. First we study the convergence behavior of the new algorithm, when the number of simulation particles goes to infinity. We show that, under appropriate assumptions on the coagulation kernel, the limit is the same as for the classical Marcus-Lushnikov process, namely the unique solution of the coagulation equation. Then a detailed numerical study is performed, testing applicability and efficiency of the algorithm. The numerical experiments illustrate the theoretical results, but also provide some insight into situations that have not yet been covered by the theory. For example, the gelation phenomenon (loss of mass in the coagulation equation) occurs when

the coagulation kernel grows sufficiently fast. A striking feature of the new algorithm is a better convergence after the gelation point, providing a tool for detecting the mass of the gel.

The paper is organized as follows. In Section 2 we introduce the basic objects of our study. Together with a weak form of equations (1.1), (1.2) we consider an equivalent equation for the flow of mass instead of the flow of concentrations. Section 3 contains the description of the new particle system. Two theorems concerning its convergence properties are given. The proofs of these theorems are collected in Section 4. In Section 5 we describe the algorithm based on the new particle system, and the direct simulation algorithm based on the Marcus-Lushnikov process that is used for comparison. In Section 6 we present results of numerical experiments. First we study the systematic error of both algorithms for several non-gelling and gelling kernels. Then we present a detailed quantitative study of the variance reduction effect resulting in a considerable efficiency gain for the new algorithm. Finally, Section 7 contains some conclusions.

2. Notation and basic equations. For a metric, locally compact and separable space E, let $C(E)$ denote the set of all continuous functions on E, $C_b(E)$ the set of all bounded $f \in C(E)$, $C_c(E)$ the set of all $f \in C(E)$ having compact support and $C_0(E)$ the set of all $f \in C(E)$ vanishing at infinity. We denote the supremum norm by $\|\cdot\|$. Let $\mathcal{M}(E)$ be the set of non-negative Borel measures on E equipped with the vague topology. A sequence $\mu_n \in \mathcal{M}(E)$ is called vaguely convergent to $\mu \in \mathcal{M}(E)$ if $\langle f, \mu_n\rangle \to \langle f, \mu\rangle \; \forall f \in C_c(E)$. For any $\mu \in \mathcal{M}(E)$ and any measurable function f we denote $\langle f, \mu\rangle = \int_E f \, d\mu$. The symbol $\xrightarrow{v}$ is used to denote vague convergence, and the symbol $\Rightarrow$ denotes weak convergence of distributions. Let $\mathbb{C}([0,\infty), \mathcal{M}(E))$ be the set of all continuous paths in $\mathcal{M}(E)$ and $\mathbb{D}([0,\infty), \mathcal{M}(E))$ denote the Skorokhod space of right continuous functions with left limits taking values in $\mathcal{M}(E)$.

Multiplication with some test function φ and integration with respect to the size variable x transform equation (1.2) into

$$
\begin{aligned}
&\int_0^\infty \varphi(x)c(t,x)\,dx \\
&\quad = \int_0^\infty \varphi(x)c_0(x)\,dx \\
&\qquad + \int_0^\infty dx\,\varphi(x)\int_0^t ds\Bigg[\tfrac{1}{2}\int_0^x K(x-y,y)c(s,x-y)\,c(s,y)\,dy \\
&\qquad\qquad - \int_0^\infty K(x,y)c(s,x)c(s,y)\,dy\Bigg] \\
&\quad = \int_0^\infty \varphi(x)c_0(x)\,dx + \int_0^t\int_0^\infty\int_0^\infty \left[\tfrac{1}{2}\varphi(x+y)-\varphi(x)\right] \\
&\qquad\qquad \times K(x,y)c(s,x)c(s,y)\,dy\,dx\,ds.
\end{aligned}
\tag{2.1}
$$

Here the identity

$$\int_0^\infty \int_0^\infty \psi(x, y)\, dy\, dx = \int_0^\infty \int_0^x \psi(x - y, y)\, dy\, dx$$

has been used. Having in mind (2.1), we consider the *coagulation equation* in the form (cf. [27], [10])

$$\begin{aligned} \langle \varphi, P(t)\rangle = \langle \varphi, P_0\rangle + \int_0^t \int_Z \int_Z \left[\tfrac{1}{2}\,\varphi(x + y) - \varphi(x)\right] \\ \times K(x, y)\, P(s, dx)\, P(s, dy)\, ds \end{aligned} \tag{2.2}$$

where $t \geq 0$ and $\varphi \in C_c(Z)$. The size space is either $Z = (0, \infty)$, corresponding to equation (1.2), or $Z = \mathbb{N}$, corresponding to equation (1.1). A function $P \in \mathbb{C}([0, \infty), \mathscr{M}(Z))$ is called a solution (with initial condition P_0) if it satisfies (2.2) and

$$\int_0^t \int_Z \int_Z K(x, y)\, P(s, dx)\, P(s, dy) < \infty \qquad \forall t > 0. \tag{2.3}$$

The coagulation kernel K is supposed to be non-negative, measurable and symmetric.

The solution $P(t, dx)$ of equation (2.2) represents the flow of concentration in the size space Z. The total mass of the system is determined as $\int_Z x\, P(t, dx)$. We call the function

$$Q(t, dx) = x\, P(t, dx), \qquad t \geq 0, \tag{2.4}$$

the mass flow and consider the *mass flow equation*

$$\begin{aligned} \langle \varphi, Q(t)\rangle = \langle \varphi, Q_0\rangle \\ + \int_0^t \int_Z \int_Z \left[\varphi(x + y) - \varphi(x)\right] \frac{K(x, y)}{y}\, Q(s, dx) Q(s, dy)\, ds \end{aligned} \tag{2.5}$$

where $t \geq 0$ and $\varphi \in C_c(Z)$. The discrete version of equation (2.5) has been used in [3] for constructing a discretized in time stochastic algorithm for equation (1.1).

A function $Q \in \mathbb{C}([0, \infty), \mathscr{M}(Z))$ is called a solution (with initial condition Q_0) if it satisfies (2.5) and

$$\int_0^t \int_Z \int_Z \frac{K(x, y)}{x\, y}\, Q(s, dx) Q(s, dy) < \infty \qquad \forall t > 0. \tag{2.6}$$

LEMMA 2.1. *Let some measure-valued functions P and Q satisfy* (2.4). *Then Q is a solution of the mass flow equation* (2.5) *if and only if P is a solution of the coagulation equation* (2.2).

PROOF. Obviously, $Q \in \mathbb{C}([0,\infty), \mathscr{M}(Z))$ iff $P \in \mathbb{C}([0,\infty), \mathscr{M}(Z))$, and (2.3) is satisfied iff (2.6) is satisfied. Let $g(x) = x$, $x \in Z$ and $\varphi \in C_c(Z)$. Note that $\langle \varphi, Q(t)\rangle = \langle \varphi\, g, P(t)\rangle$. Using symmetry, one obtains

$$\begin{aligned}
&\int_Z \int_Z \left[\frac{1}{2}\,\varphi(x+y)\,(x+y) - \varphi(x)\,x\right] K(x,y)\,P(s,dx)\,P(s,dy)\\
&\quad = \int_Z \int_Z \left[\varphi(x+y)\,x - \varphi(x)\,x\right] \frac{K(x,y)}{x\,y}\,Q(s,dx)\,Q(s,dy)\\
&\quad = \int_Z \int_Z \left[\varphi(x+y) - \varphi(x)\right] \frac{K(x,y)}{y}\,Q(s,dx)\,Q(s,dy),
\end{aligned}$$

and the equivalence follows.

3. Mass flow particle system. In this section we introduce a sequence of stochastic particle systems and study its approximation properties regarding the solution of equation (2.5).

Suppose

$$K(x,y) \le h(x)h(y) \qquad \forall x, y \in Z, \tag{3.1}$$

where $h \in C(Z)$ is positive and

$$\frac{h(x)}{x} \qquad \text{is non-increasing.} \tag{3.2}$$

Let $b_N > 0$, $\beta > 0$, and define

$$\mathscr{M}_\beta^N = \left\{ p = \frac{1}{N}\sum_{i=1}^n \delta_{x_i} \in \mathscr{M}(Z) : x_i \in Z \cap (0, b_N], \int_Z \frac{h(x)}{x}\,p(dx) \le \beta \right\}, \tag{3.3}$$

where δ denotes the Dirac measure. We introduce the *generator*

$$\mathscr{G}^N\Phi(p) = \frac{1}{N}\sum_{1\le i,j\le n} \Big[\Phi(J(p,x_i,x_j)) - \Phi(p)\Big]\frac{K(x_i,x_j)}{x_j},\ \Phi \in C_b(\mathscr{M}_\beta^N), \tag{3.4}$$

where

$$J(p,x,y) = \begin{cases} p - \dfrac{1}{N}\,\delta_x + \dfrac{1}{N}\,\delta_{x+y}, & x+y \le b_N,\\[2ex] p - \dfrac{1}{N}\,\delta_x, & x+y > b_N. \end{cases} \tag{3.5}$$

Note that condition (3.2) guarantees

$$J(p,x,y) \in \mathscr{M}_\beta^N. \tag{3.6}$$

By (3.1) and the truncation in (3.3) one obtains the estimate

$$\sup_{p\in\mathscr{M}_\beta^N} \left|\mathscr{G}^N\Phi(p)\right| \le 2\,\|\Phi\| N \sup_{p\in\mathscr{M}_\beta^N} \int_Z \int_Z \frac{K(x,y)}{y}\,p(dx)p(dy) \le 2\|\Phi\| N b_N \beta^2.$$

Thus the generator $\mathcal{G}^N$ is bounded for every N, and a corresponding jump process U^N exists for any initial distribution on the state space $\mathcal{M}_\beta^N$ (cf. [11], page 162). Since $\mathcal{M}_\beta^N$ is a subset of

$$\mathcal{M}_\beta = \left\{ p \in \mathcal{M}(Z) : \int_Z \frac{h(x)}{x}\, p(dx) \le \beta \right\}, \tag{3.7}$$

U^N can be regarded as a stochastic process with trajectories in $\mathbb{D}([0,\infty), \mathcal{M}_\beta)$. The basic approximation properties of the sequence U^N are given by the following two theorems.

THEOREM 3.1. *Suppose the coagulation kernel K satisfies* (3.1), (3.2). *Then $\{U^N\}_{N=1}^\infty$ is relatively compact in $\mathbb{D}([0,\infty), \mathcal{M}_\beta)$ and for any weak limit U,*

$$P\left(U \in \mathbb{C}([0,\infty), \mathcal{M}_\beta)\right) = 1. \tag{3.8}$$

THEOREM 3.2. *Suppose the coagulation kernel $K \in C(Z \times Z)$ satisfies* (3.1), (3.2) *and*

$$\lim_{x+y\to\infty} \frac{K(x,y)}{h(x)\,h(y)} = 0. \tag{3.9}$$

Let

$$b_N \to \infty \tag{3.10}$$

and

$$U_0^N \Rightarrow Q_0 \in \mathcal{M}_\beta. \tag{3.11}$$

Then any weak limit point of $\{U^N\}_{N=1}^\infty$ solves almost surely the mass flow equation (2.5) *with initial condition Q_0.*

Note that Theorems 3.1, 3.2 imply existence of solutions to the mass flow equation (2.5) and, via Lemma 2.1, to the coagulation equation (2.2). This existence result is closely related to [27], Theorem 4.1. Though the notions of solution are slightly different, the assumptions on the initial condition and the coagulation kernel are the same. In particular, condition (3.2) is equivalent to

$$\frac{h(\lambda x)}{\lambda x} \le \frac{h(x)}{x} \qquad \forall x > 0,\ \lambda \ge 1,$$

that is, sublinearity of h,

$$h(\lambda x) \le \lambda\, h(x) \qquad \forall x > 0,\ \lambda \ge 1.$$

However, our purpose is not a new existence theorem but the justification of the approximation properties of the mass flow process.

4. Proofs.

LEMMA 4.1. *Let $\mu_n, \mu \in \mathscr{M}(E)$ and $G \in C(E)$ non-negative. If $\mu_n \xrightarrow{v} \mu$, then*

$$\langle G, \mu\rangle \le \liminf_n \langle G, \mu_n\rangle. \tag{4.1}$$

PROOF. Define $\nu_n, \nu \in \mathscr{M}(E)$ by

$$\nu_n(dx) = G(x)\,\mu_n(dx), \qquad \nu(dx) = G(x)\,\mu(dx).$$

Let $\varphi \in C_c(E)$. Since $\varphi G \in C_c(E)$, we obtain

$$\langle \varphi, \nu_n\rangle = \langle \varphi G, \mu_n\rangle \to \langle \varphi G, \mu\rangle = \langle \varphi, \nu\rangle$$

so that $\nu_n \xrightarrow{v} \nu$, and (4.1) follows from [4], Lemma 30.3. □

REMARK 4.2. The set $\mathscr{M}_\beta$ [cf. (3.7)] is compact, since it is relatively compact, according to [4, Theorem 31.2], and closed, by (4.1).

Let $\{\psi_k\}_{k=1}^\infty \subset C_c(Z)$ be dense with respect to uniform convergence. For any $m \in \mathbb{N}$ choose

$$e_m \in C_c(Z) : 0 \le e_m \le 1, \qquad e_m(x) = 1,\ x \in Z \cap [1/m, m]. \tag{4.2}$$

Reorder the elements of the countable set

$$\{\psi_k : k \in \mathbb{N}\} \cup \{\psi_k \cdot e_m : k, m \in \mathbb{N}\} \cup \{e_m : m \in \mathbb{N}\} \tag{4.3}$$

and denote them by $\{\varphi_k\}_{k=1}^\infty$. Then

$$d_v(\mu, \nu) = \sum_{k=1}^\infty \frac{1}{2^k} \min\{1, |\langle \varphi_k, \mu\rangle - \langle \varphi_k, \nu\rangle|\}, \qquad \mu, \nu \in \mathscr{M}(Z), \tag{4.4}$$

is a complete metric generating the vague topology on $\mathscr{M}(Z)$ so that $(\mathscr{M}(Z), d_v)$ is Polish (cf. [4], Theorem 31.5). By Remark 4.2 the set $\mathscr{M}_\beta$ is closed so that the Skorokhod space $\mathbb{D}([0,\infty), \mathscr{M}_\beta)$ is also Polish.

For $\varphi \in C_c(Z)$ define $\Phi \in C_b(\mathscr{M}_\beta^N)$ by $\Phi(p) = \langle \varphi, p\rangle$ and denote $\mathscr{G}_N(\varphi, p) = \mathscr{G}^N\Phi(p)$ (cf. (3.4)) so that

$$\mathscr{G}_N(\varphi, p) = N \int_Z \int_Z [\langle \varphi, J(p, x, y)\rangle - \langle \varphi, p\rangle] \frac{K(x, y)}{y}\, p(dx)\, p(dy). \tag{4.5}$$

The corresponding martingale is

$$M_\varphi^N(t) = \langle \varphi, U^N(t)\rangle - \langle \varphi, U^N(0)\rangle - \int_0^t \mathscr{G}_N(\varphi, U^N(s))\, ds. \tag{4.6}$$

LEMMA 4.3. *Suppose the coagulation kernel K satisfies* (3.1), (3.2). *Then, for $t \geq 0$ and $\varphi \in C_c(Z)$,*

$$\sup_N \mathbb{E} \sup_{s \leq t} \left| \mathscr{G}_N(\varphi, U^N(s)) \right| < \infty \tag{4.7}$$

and

$$\lim_{N \to \infty} \mathbb{E} \sup_{s \leq t} \left| M_\varphi^N(s) \right| = 0. \tag{4.8}$$

PROOF. We introduce the notation

$$B(\varphi) = \sup\{x \in Z : \varphi(x) \neq 0\}, \quad \varphi \in C_c(Z). \tag{4.9}$$

By (4.5), (3.5) one obtains

$$\begin{aligned} \left| \mathscr{G}_N(\varphi, U^N(s)) \right| &\leq \beta^2 \sup_{x,y \in Z} \Big[x \max\Big(|\varphi(x)|, |\varphi(x) - \varphi(x+y)| \Big) \Big] \\ &\leq 2\,\beta^2\, B(\varphi)\, \|\varphi\|, \end{aligned}$$

and (4.7) follows. Since $\Phi^2 \in C_b(\mathscr{M}_\beta^N)$, we obtain

$$\begin{aligned} \mathbb{E}\left[M_\varphi^N(t) \right]^2 &= \mathbb{E} \int_0^t \left[\mathscr{G}^N \Phi^2 - 2\,\Phi\, \mathscr{G}^N \Phi \right] (U^N(s))\, ds \\ &= N\, \mathbb{E} \int_0^t \int_Z \int_Z \Big[\langle \varphi, J(U^N(s), x, y) \rangle - \langle \varphi, U^N(s) \rangle \Big]^2 \\ &\qquad \times \frac{K(x,y)}{y}\, U^N(s, dx)\, U^N(s, dy)\, ds \\ &\leq \frac{1}{N}\, \mathbb{E} \int_0^t \int_Z \int_Z \Big[(\varphi(x+y) - \varphi(x))^2 + \varphi(x)^2 \Big] \\ &\qquad \times \frac{K(x,y)}{y}\, U^N(s, dx)\, U^N(s, dy)\, ds \\ &\leq \frac{5\,\beta^2\, B(\varphi)\, \|\varphi\|^2\, t}{N}. \end{aligned}$$

Applying Doob's inequality, we obtain

$$\left(\mathbb{E} \sup_{s \leq t} \left| M_\varphi^N(s) \right| \right)^2 \;\leq\; 4\, \mathbb{E}\left[M_\varphi^N(t) \right]^2,$$

and thus (4.8). □

PROOF OF THEOREM 3.1. We prove the relative compactness of the sequence U^N using a criterion from [11], Corollary 3.7.4. By Remark 4.2, the first condition of the criterion is fulfilled. The second condition is stated in

terms of the following modulus of continuity. For $y \in \mathbb{D}([0,\infty), \mathscr{M}(Z))$, $\delta > 0$ and $T > 0$, define

$$w(y,\delta,T) = \inf_{\{t_i\}} \max_i \sup_{s,t\in[t_{i-1},t_i)} d_v(y(s),y(t)),$$

where $\{t_i\}$ ranges over all partitions of the form $0 = t_0 < t_1 < \cdots < t_{n-1} < T \le t_n$ with $\min_{1\le i\le n}(t_i - t_{i-1}) > \delta$ and $n \ge 1$. To prove relative compactness, it remains to show that

$$\forall\, T, \eta > 0, \quad \exists \delta > 0 : \limsup_{N\to\infty} P(w(U^N,\delta,T) \ge \eta) \le \eta.$$

Notice that, for $\delta < \Delta t$ and $t_i = i\,\Delta t$,

$$w(y,\delta,T) \le 2 \max_{t_i<T} \sup_{s\in[t_i,t_{i+1})} d_v(y(s),y(t_i)).$$

Thus, it is enough to show

$$\limsup_{N\to\infty} P\left(\max_{t_i<T} \sup_{s\in[t_i,t_{i+1})} d_v(U^N(s),U^N(t_i)) \ge \eta\right) \le \eta, \tag{4.10}$$

for sufficiently small Δt. By definition (4.4) and the martingale representation (4.6), for $t \le s$, we obtain

$$\begin{aligned} &d_v(U^N(s),U^N(t)) \\ &\quad= \sum_{k=1}^{\infty} \frac{1}{2^k} \min\left\{1, \left|\langle\varphi_k, U^N(s)\rangle - \langle\varphi_k, U^N(t)\rangle\right|\right\} \\ &\quad\le \sum_{k=1}^{\infty} \frac{1}{2^k} \min\left\{1, \left|M^N_{\varphi_k}(s) - M^N_{\varphi_k}(t)\right| + \int_t^s \left|\mathscr{G}_N(\varphi_k, U^N(r))\right| dr\right\}. \end{aligned}$$

Applying Chebyschev's inequality gives

$$\begin{aligned} &P\left(\max_{t_i<T} \sup_{s\in[t_i,t_{i+1})} d_v(U^N(s),U^N(t_i)) \ge \eta\right) \\ &\quad\le P\left(\max_{t_i<T} \sup_s \sum_{k=1}^{\infty} \frac{1}{2^k} \min\left\{1, \left|M^N_{\varphi_k}(s) - M^N_{\varphi_k}(t_i)\right| \right.\right. \\ &\qquad\qquad \left.\left. + \int_{t_i}^s \left|\mathscr{G}_N(\varphi_k, U^N(r))\right| dr\right\} \ge \eta\right) \\ &\quad\le \frac{1}{\eta} \sum_{k=1}^{\infty} \frac{1}{2^k} \min\left\{1, 2\,\mathbb{E} \sup_{s\le T+\Delta t} \left|M^N_{\varphi_k}(s)\right| + \Delta t\, \mathbb{E} \sup_{s\le T+\Delta t} \left|\mathscr{G}_N(\varphi_k, U^N(s))\right|\right\}. \end{aligned}$$

Using Lemma 4.3, we obtain (4.10) for sufficiently small Δt, and the proof of relative compactness is complete. The vague distance of two consecutive states

in $\mathscr{M}_\beta^N$ is bounded by

$$\sum_{k=1}^{\infty} \frac{1}{2^k} \min\left\{1, \frac{2\,\|\varphi_k\|}{N}\right\}$$

and (3.8) follows from [11], Theorem 3.10.2(a).

To prepare the proof of Theorem 3.2 we introduce the notation

$$\mathscr{G}(\varphi, p) = \int_Z \int_Z [\varphi(x+y) - \varphi(x)]\, \frac{K(x,y)}{y}\, p(dx)\, p(dy) \tag{4.11}$$

and

$$M_\varphi(q,t) = \langle \varphi, q(t)\rangle - \langle \varphi, q(0)\rangle - \int_0^t \mathscr{G}(\varphi, q(s))\, ds, \tag{4.12}$$

where $\varphi \in C_c(Z)$, $p \in \mathscr{M}_\beta$ and $q \in \mathbb{D}([0,\infty), \mathscr{M}_\beta)$. With these notations, the mass flow equation (2.5) takes the form $M_\varphi(q,t) = 0$.

LEMMA 4.4. *Suppose the coagulation kernel $K \in C(Z \times Z)$ satisfies* (3.1), (3.2) *and* (3.9). *Let $\varphi \in C_c(Z)$, $q_n \in \mathbb{D}([0,\infty), \mathscr{M}_\beta)$ and $q \in \mathbb{C}([0,\infty), \mathscr{M}_\beta)$. If $q_n \to q$ w.r.t. Skorokhod topology then*

$$M_\varphi(q_n, t) \to M_\varphi(q,t), \qquad t \ge 0. \tag{4.13}$$

PROOF. Given $\delta > 0$, we represent the kernel in the form $K = K_1 + K_2$, where $K_1 \in C_c(Z \times Z)$ and $0 \le K_2 \le K$ is supported on

$$\Big\{(x,y) :\ x \le \delta\Big\} \cup \Big\{(x,y) :\ y \le \delta\Big\} \cup \Big\{(x,y) :\ x + y \ge \delta^{-1}\Big\}.$$

Introduce the notation

$$g_i(x,y) = [\varphi(x+y) - \varphi(x)]\, \frac{K_i(x,y)}{y}, \qquad i = 1, 2.$$

For any $p \in \mathscr{M}_\beta$, we obtain [cf. (4.9)]

$$\int\int_{x\le\delta} |g_2(x,y)|\, p(dx)\, p(dy) \le 2\,\|\varphi\|\,\delta\,\beta^2,$$

$$\int\int_{y\le\delta} |g_2(x,y)|\, p(dx)\, p(dy) \le B(\varphi) \sup_{|x-y|\le\delta} |\varphi(x) - \varphi(y)|\ \beta^2$$

and

$$\int\int_{x+y\ge\delta^{-1}} |g_2(x,y)|\, p(dx)\, p(dy) \le 2\,\|\varphi\|\, B(\varphi) \sup_{x+y\ge\delta^{-1}} \frac{K(x,y)}{h(x)\,h(y)}\ \beta^2.$$

Thus, given $\varepsilon > 0$, one can find $\delta > 0$ so that

$$\int_Z \int_Z |g_2(x,y)|\, p(dx)\, p(dy) \le \varepsilon, \qquad \forall p \in \mathscr{M}_\beta. \tag{4.14}$$

Here condition *(3.9)* has been used. Let $p_n, p \in \mathscr{M}_\beta$ such that $p_n \xrightarrow{v} p$. Then $p_n \times p_n \xrightarrow{v} p \times p$ and

$$\int_Z \int_Z g_1(x, y)\, p_n(dx)\, p_n(dy) \to \int_Z \int_Z g_1(x, y)\, p(dx)\, p(dy). \tag{4.15}$$

Using (4.14) and (4.15), we obtain [cf. (4.11)] $limsup_n\, |\mathscr{G}(\varphi, p_n) - \mathscr{G}(\varphi, p)| \le 2\varepsilon$ so that

$$\lim_n \mathscr{G}(\varphi, p_n) = \mathscr{G}(\varphi, p). \tag{4.16}$$

According to (3.1) [cf. (4.9)],

$$\left|\mathscr{G}(\varphi, q_n(s))\right| \le 2\, \|\varphi\|\, B(\varphi)\, \beta^2. \tag{4.17}$$

Since q is continuous, $q_n(s) \xrightarrow{v} q(s)$ for every s. Finally, (4.16), (4.17) and the dominated convergence theorem imply (4.13). □

LEMMA 4.5. *Suppose the coagulation kernel satisfies* (3.1) *and* (3.2). *If* $q \in \mathbb{D}([0, \infty), \mathscr{M}_\beta)$ *satisfies equation* (2.5) *for all* φ_k [*cf.* (4.2), (4.3)] *then* q *satisfies equation* (2.5) *for all* $\varphi \in C_c(Z)$.

PROOF. For any $\varphi \in C_c(Z)$ there exist $m > 1$ and a subsequence $\{\varphi_{k_n}\}_{n=1}^{\infty}$ such that

$$\|\varphi - \varphi_{k_n}\| \to 0 \quad \text{and} \quad \{x : \varphi_{k_n}(x) \ne 0\} \subset [1/m, m]. \tag{4.18}$$

Drop the index n. By the dominated convergence theorem

$$\langle \varphi_k, q(t)\rangle \to \langle \varphi, q(t)\rangle, \qquad t \ge 0. \tag{4.19}$$

Consider

$$\begin{aligned} g_k(x, y) &= [\varphi_k(x + y) - \varphi_k(x)]\, \frac{K(x, y)}{y} \\ &\to [\varphi(x + y) - \varphi(x)]\, \frac{K(x, y)}{y} = g(x, y). \end{aligned}$$

Using [cf. (4.18)]

$$|g_k(x, y)| \le 2\, m\, \sup_k \|\varphi_k\| \frac{h(x)}{x} \frac{h(y)}{y}, \tag{4.20}$$

the dominated convergence theorem implies

$$\begin{aligned} &\int_Z \int_Z g_k(x, y) q(s, dx) q(s, dy) \\ &\qquad \to \int_Z \int_Z g(x, y)\, q(s, dx)\, q(s, dy), \qquad s \ge 0. \end{aligned} \tag{4.21}$$

Moreover, one obtains from (4.20) that

$$\sup_k \sup_{s \le t} \int_Z \int_Z g_k(x, y)\, q(s, dx)\, q(s, dy) \;\le\; 2\, m\, \sup_k \|\varphi_k\|\, \beta^2.$$

Thus (4.19), (4.21) and a further application of the dominated convergence theorem give

$$\begin{aligned}\langle \varphi, q(t)\rangle &= \lim_k \langle \varphi_k, q(t)\rangle \\ &= \lim_k \left[\langle \varphi_k, q(0)\rangle + \int_0^t \int_Z \int_Z g_k(x,y)\, q(s,dx)\, q(s,dy)\, ds \right] \\ &= \langle \varphi, q(0)\rangle + \int_0^t \int_Z \int_Z g(x,y)\, q(s,dx)\, q(s,dy)\, ds.\end{aligned}$$

This completes the proof. □

PROOF OF THEOREM 3.2. Let $\varphi \in C_c(Z)$. Note that [cf. (4.5), (3.5), (4.11)]

$$\mathcal{G}_N(\varphi, p) = \mathcal{G}(\varphi, p) - \int\int_{x+y>b_N} \varphi(x+y)\, \frac{K(x,y)}{y}\, p(dx)\, p(dy).$$

By (4.12), (4.6) this representation implies

$$\begin{aligned}\mathbb{E}\left|M_\varphi(U^N,t)\right| &\le \mathbb{E}\left|M_\varphi^N(t)\right| \\ &\quad + \mathbb{E}\int_0^t \int\int_{x+y>b_N} |\varphi(x+y)|\, \frac{K(x,y)}{y}\, U^N(s,dx)\, U^N(s,dy)\, ds \\ &\le \mathbb{E}\left|M_\varphi^N(t)\right| + 2\,\|\varphi\|\, B(\varphi)\, t\, \beta^2 \sup_{x+y>b_N} \frac{K(x,y)}{h(x)\,h(y)}.\end{aligned}$$

According to (4.8) and assumptions (3.9), (3.10), we conclude that

$$\lim_{N\to\infty} \mathbb{E}\left|M_\varphi(U^N,t)\right| = 0, \qquad t \ge 0. \tag{4.22}$$

Suppose $U^{N_n} \Rightarrow U$. By (3.8) and Lemma 4.4, we obtain $M_\varphi(U^{N_n}, t) \Rightarrow M_\varphi(U,t)$. An application of Fatou's lemma (cf. [11], page 492) and (4.22) imply

$$\mathbb{E}\left|M_\varphi(U,t)\right| = 0. \tag{4.23}$$

Taking into account (3.8) we obtain $M_\varphi(U,\cdot) \in \mathbb{C}([0,\infty),\mathbb{R})$ a.e. so that (4.23) implies

$$M_\varphi(U,t) = 0 \qquad \forall t \ge 0, \text{ a.e.}$$

and, by Lemma 4.5,

$$M_\varphi(U,t) = 0 \qquad \forall t \ge 0, \quad \forall \varphi \in C_c(Z), \text{ a.e.}$$

According to (3.11) we have $U(0) = Q_0$ almost everywhere. Condition (2.6) follows from (3.1) and (3.7) so that U is almost surely a solution of the mass flow equation with initial condition Q_0. □

5. Description of the algorithms. The stochastic process studied in the previous sections provides a random approximate solution to the mass flow equation (2.5) and, via (2.4), also to the coagulation equation (2.2). If the current state of the process is represented by particles $x_1(t), \dots, x_{n(t)}(t)$, then *functionals of the solution* P to equation (2.2) are approximated as

$$I := \int_Z \varphi(x)\, P(t, dx) \sim \frac{1}{N} \sum_{i=1}^{n(t)} \frac{\varphi(x_i(t))}{x_i(t)} =: \xi^N, \tag{5.1}$$

for some test function φ and $t \geq 0$. In particular, the sum concentrations

$$C(t, a, b) = P(t, [a, b]), \qquad 0 < a < b, \tag{5.2}$$

and the moments

$$m_\delta(t) = \int_Z x^\delta\, P(t, dx), \qquad \delta \geq 0, \tag{5.3}$$

are suitable functionals for our subsequent numerical studies. The *numerical algorithm* consists of:

- generating trajectories of the process and
- calculating estimators ξ^N for various functionals I of the solution.

The standard stochastic model related to the coagulation equation (2.2) is the Marcus-Lushnikov process mentioned in the Introduction. Here two different clusters of size x and y coagulate to a single cluster of size $x+y$ with rate $K(x, y)$. If the current state of the process is represented by particles $y_1(t), \dots, y_{n(t)}(t)$, then functionals are approximated by (contrast this with (5.1))

$$\int_Z \varphi(x)\, P(t, dx) \sim \frac{1}{N} \sum_{i=1}^{n(t)} \varphi(y_i(t)) =: \tilde{\xi}^N. \tag{5.4}$$

In the following subsections we first describe details of the algorithm based on the mass flow particle system, then we introduce the standard direct simulation algorithm (used later for comparison), and finally we discuss the issue of comparing stochastic algorithms with respect to their efficiency.

5.1. *The mass flow algorithm.* The mass flow process determined by the generator (3.4), (3.5) is a pure jump process. For an efficient generation of trajectories we replace the coagulation kernel by the majorant product kernel $h(x)\, h(y)$ [cf. (3.1)] and introduce fictitious jumps. This leads to an easy calculation of the time step and to an independent generation of the collision partners. For more details of this common numerical approach we refer to [9].

The resulting simulation procedure is as follows:

1. Generate the initial state $(x_1, \ldots, x_n)$ [cf. (3.3)].
2. Wait an exponentially distributed time step τ with parameter
$$\frac{1}{N} \sum_{i=1}^{n} h(x_i) \sum_{j=1}^{n} \frac{h(x_j)}{x_j}.$$
3. Choose the first collision partner i according to the distribution
$$\frac{h(x_i)}{\sum_{k=1}^{n} h(x_k)}, \qquad i = 1, \ldots, n, \tag{5.5}$$
and the second collision partner j independently according to the distribution
$$\frac{\frac{h(x_j)}{x_j}}{\sum_{k=1}^{n} \frac{h(x_k)}{x_k}}, \qquad j = 1, \ldots, n. \tag{5.6}$$
4. With probability
$$\frac{K(x_i, x_j)}{h(x_i)\, h(x_j)},$$
remove x_i and, if $x_i + x_j \le b_N$, add $x_i + x_j$.
5. Go to step 2.

The generalization of this procedure to other majorant kernels, like sums of products, is straightforward.

Note that, for the special choices $h(x) = c$ and $h(x) = c\,x$, $c > 0$, one of the distributions (5.5) and (5.6) becomes uniform. In general, these distributions are of the form
$$\frac{q_i}{\sum_{j=1}^{n} q_j}, \qquad i = 1, \ldots, n,$$
where the weights satisfy $0 < q_i \le B$, and can be generated via an acceptance rejection technique. Namely, the weights q_i are ordered according to their size in γ groups
$$(0, B_1], (B_1, B_2], \ldots, (B_{\gamma-1}, B_\gamma], \qquad 0 < B_1 < \ldots < B_{\gamma-1} < B_\gamma = B.$$
Then a group index $1 \le j \le \gamma$ is generated according to the group weights and a weight index i is chosen uniformly among all weight indices in the jth group. With probability $\frac{q_i}{B_j}$ the weight index is accepted else a new weight index is chosen within the same group.

We call the above simulation procedure combined with this acceptance rejection technique *mass flow algorithm* (*MFA*).

5.2. *The direct simulation algorithm.* For an efficient generation of trajectories of the Marcus-Lushnikov process, we can apply similar techniques (introduction of fictitious jumps, acceptance-rejection technique) as for the mass flow process. For sake of completeness, we describe the resulting algorithm for the special choice of the product majorant kernel $h(x)h(y)$:

1. Generate the initial state $(y_1, \dots, y_n)$.
2. Wait an exponentially distributed time step τ with parameter
$$\frac{1}{N}\left(\sum_{i=1}^{n} h(y_i)\right)^2.$$
3. Choose the collision partners i and j independently according to the distribution
$$\frac{h(y_l)}{\sum_{k=1}^{n} h(y_k)}, \qquad l = 1, \dots, n.$$
4. If $i = j$ then go to step 2. Else with probability
$$\frac{K(y_i, y_j)}{h(y_i)\, h(y_j)}$$
remove the clusters y_i and y_j and add the cluster $y_i + y_j$.
5. Go to step 2.

Due to the physical meaning of the Marcus-Lushnikov process we call the above simulation procedure *direct simulation algorithm* (*DSA*).

5.3. *Comparison of stochastic algorithms.* To compare the efficiency of two algorithms means to compare the effort, which has to be spent in order to reach a given level of accuracy. The quality of the algorithms depends on the *convergence properties* of the estimators defined in (5.1), (5.4) (characterized by the expectations $E\,\xi^N$, $E\,\tilde{\xi}^N$ and variances Var ξ^N, Var $\tilde{\xi}^N$), and on the *mean computational effort* per trajectory r^N or $\tilde{r}^N$. Averaging over R independent trajectories is used to get estimates of those quantities.

Note that properties as

- convergence of $E\,\xi^N$ and $E\,\tilde{\xi}^N$ to I, or
- convergence of Var ξ^N and Var $\tilde{\xi}^N$ to zero,

depend only on the underlying processes. However, the effort depends on the procedure for generating trajectories, in particular on the choice of the majorant kernels, and on the implementation of this procedure on the computer.

Let the *systematic error*

$$e^N_{\text{sys}} = \left|E\,\xi^N - I\right| \qquad \text{and} \qquad \tilde{e}^{\tilde{N}}_{\text{sys}} = \left|E\,\tilde{\xi}^{\tilde{N}} - I\right|$$

take the value $\varepsilon > 0$, for some parameters $N = N(\varepsilon)$ and $\tilde{N} = \tilde{N}(\varepsilon)$. The length of the confidence intervals, which are constructed using empirical values, is proportional to

$$\sqrt{\frac{\operatorname{Var}\,\xi^N}{R}} \qquad \text{and} \qquad \sqrt{\frac{\operatorname{Var}\,\tilde{\xi}^{\tilde{N}}}{\tilde{R}}}.$$

These *statistical error* bounds take the value ε when

$$R = \frac{\operatorname{Var}\,\xi^N}{\varepsilon^2} \qquad \text{or} \qquad \tilde{R} = \frac{\operatorname{Var}\,\tilde{\xi}^{\tilde{N}}}{\varepsilon^2}$$

trajectories are used, so that the corresponding effort is

$$\frac{1}{\varepsilon^2}\, r^N \operatorname{Var}\,\xi^N \qquad \text{or} \qquad \frac{1}{\varepsilon^2}\, \tilde{r}^{\tilde{N}} \operatorname{Var}\,\tilde{\xi}^{\tilde{N}}.$$

Finally, the fraction

$$\kappa = \frac{\tilde{r}^{\tilde{N}} \operatorname{Var}\,\tilde{\xi}^{\tilde{N}}}{r^N \operatorname{Var}\,\xi^N} \tag{5.7}$$

gives the *gain factor* when using ξ^N instead of $\tilde{\xi}^{\tilde{N}}$.

6. Numerical results. We restrict our numerical investigation to the discrete coagulation equation (1.1) with monodisperse initial condition

$$c(0,1) = 1, \qquad c(0,k) = 0, \;\; k \geq 2, \tag{6.1}$$

and start the MFA and the DSA (defined in the previous section) with the initial state

$$x_i(0) = y_i(0) = 1, \qquad i = 1, \ldots, N.$$

Kernels satisfying

$$K(i,j) \leq c\,(i+j), \qquad c > 0,$$

provide unique mass-conserving solutions (cf. [19], [27]). In this class we consider the kernel

$$K(i,j) = \sqrt{\frac{1}{i} + \frac{1}{j}}\,\left(i^{1/3} + j^{1/3}\right)^2, \tag{6.2}$$

which corresponds to the so-called free molecular collision regime and is used in practical studies of aerosol dynamics [23]. The kernel (6.2) satisfies the conditions of Theorems 3.1, 3.2 so that convergence for MFA follows.

One of the most interesting phenomena related to coagulation processes is the fact that sufficiently fast increasing coagulation kernels lead to solutions exhibiting gelation, that is, a loss of initial mass in finite time (cf. [2], Section 2.3, [20]). Define the *gelation time* for a solution P of the coagulation equation by [cf. (5.3)]

$$t_g = \inf\left\{t \geq 0 : m_1(t) < m_1(0)\right\} \tag{6.3}$$

and call the solution gelling if $t_g < \infty$. A kernel is called gelling if there is a gelling solution. The condition

$$\exists\, c > 0,\ 0.5 < \varepsilon < 1 : c\,(ij)^{\varepsilon} \le K(i, j) \quad \text{and} \quad K(i, j) = o(ij)$$

is sufficient to provide existence of gelling solutions [20], Corollary 1. Under some additional assumptions, uniqueness has been proved up to the gelation point [27], so that convergence follows from Theorems 3.1, 3.2 for MFA, and related results for DSA. Note that convergence of the algorithms after the gelation time has not been established so far. However, if they converge, then to a solution. As an example in this class of gelling kernels we consider the product kernel

$$K(i, j) = (i\ j)^{\alpha}, \qquad 0.5 < \alpha < 1. \tag{6.4}$$

A kernel satisfying

$$K(c\,i, c\,j) = c^{\gamma} K(i, j) \qquad \forall c > 0, \tag{6.5}$$

is called *homogeneous* with exponent γ. Such kernels are expected to be gelling if $\gamma > 1$. Many kernels of practical relevance satisfy (6.5). In particular, the kernel (6.2) is homogeneous with exponent $\gamma = 1/6$. Note that the kernel (6.4) is homogeneous with $\gamma = 2\,\alpha$. We also consider the kernel

$$K(i, j) = \frac{2(ij)^{\gamma}}{(i + j)^{\gamma} - i^{\gamma} - j^{\gamma}}, \qquad 1 < \gamma \le 2, \tag{6.6}$$

which is homogeneous with exponent γ.

The kernel (6.6) takes the form

$$K(i, j) = i\ j, \tag{6.7}$$

if $\gamma = 2$. In this case the unique solution to the discrete coagulation equation (1.1) with monodisperse initial condition (6.1) is given by

$$c(t, k) = \begin{cases} \dfrac{k^{k-2}}{k!}\, t^{k-1}\, \exp(-kt), & 0 \le t \le 1, \\ \dfrac{k^{k-2}}{k!}\, \exp(-k)\, t^{-1}, & 1 < t \end{cases} \tag{6.8}$$

and the mass by

$$m_1(t) = \begin{cases} 1, & 0 \le t \le 1, \\ t^{-1}, & 1 < t \end{cases} \tag{6.9}$$

so that $t_g = 1$. According to [1], it is expected that $t_g = 1$ for all kernels of the form (6.6). For the multiplicative kernel (6.7) it has been proved in [6] that the Marcus-Lushnikov process converges to

$$\hat{c}(t, k) = \frac{k^{k-2}}{k!}\, t^{k-1}\, \exp(-kt), \qquad t \ge 0, \tag{6.10}$$

which agrees with (6.8) only in the pre-gelation phase. Its mass can be calculated from

$$\hat{m}_1(t) = \begin{cases} 1, & 0 \le t \le 1, \\ \dfrac{t^*}{t}, & 1 < t, \end{cases} \tag{6.11}$$

where $t^* = t^*(t)$ is determined by the equation

$$t^* \exp(-t^*) = t \exp(-t), \qquad t^* \in (0, 1), \ t > 1.$$

The main purpose of the numerical examples is to illustrate the *new features* of the MFA compared to the DSA. There are three main aspects:

- the systematic error of MFA is significantly smaller;
- MFA is convenient for calculations beyond the gelation point;
- MFA is more efficient for many functionals due to considerable variance reduction.

We first analyze the convergence behavior of the MFA and DSA for non-gelling and gelling kernels. Then we consider the issue of efficiency.

6.1. *Systematic error and convergence in the non-gelling case.* The convergence behavior of both algorithms for the kernel (6.2) is illustrated in Figure 1. Since exact solutions are not available for this kernel, the results for the DSA started with 10^8 monomer particles are used as a reference solution (dashed lines). Results are shown for the functional $C(t, 100, 200)$ [cf. (5.2)] in the upper plots, and for the second moment $m_2(t)$ [cf. (5.3)] in the lower plots. Data for DSA (left plots) are given for $N = 2^9, 2^{10}, \ldots, 2^{13}$ initial monomers. Data for MFA (right plots) were obtained for $N = 16$ initial particles and $b_N = 1000$. Note that the influence of the truncation parameter b_N is negligible if it is chosen sufficiently large.

Figure 1 provides a first observation of the fact that MFA has much smaller systematic error. This effect is partly due to the decrease of the particle number in DSA. For the kernel (6.2) the initial particle number is reduced by a factor 200 at the end of the considered time interval. However, the results for MFA with $N = 16$ particles are in better agreement with the reference trajectory than the results for DSA even with $N = 2^{12} > 16 \times 200$ (having more particles at the end). In the following we will investigate this effect in more detail.

We consider the second moment $m_2(t)$. Curves for the quantities $N\, e_{sys}^N(t)$ and $\tilde{N}\, \tilde{e}_{sys}^{\tilde{N}}(t)$ are shown in Figure 2 for DSA with $\tilde{N} = 2^{11}$ (solid) and $\tilde{N} = 2^{13}$ (dashed), and for MFA with $N = 16$ (solid) and $N = 64$ (dashed). These results indicate that the order of convergence is the same for both algorithms. Note that such numerical investigations are rather limited, since the confidence intervals have to be kept very small in order to detect the systematic error sufficiently accurately.

Now we take into account the number of particles, which decreases drastically for DSA. The question is whether, at a fixed time t, the systematic error

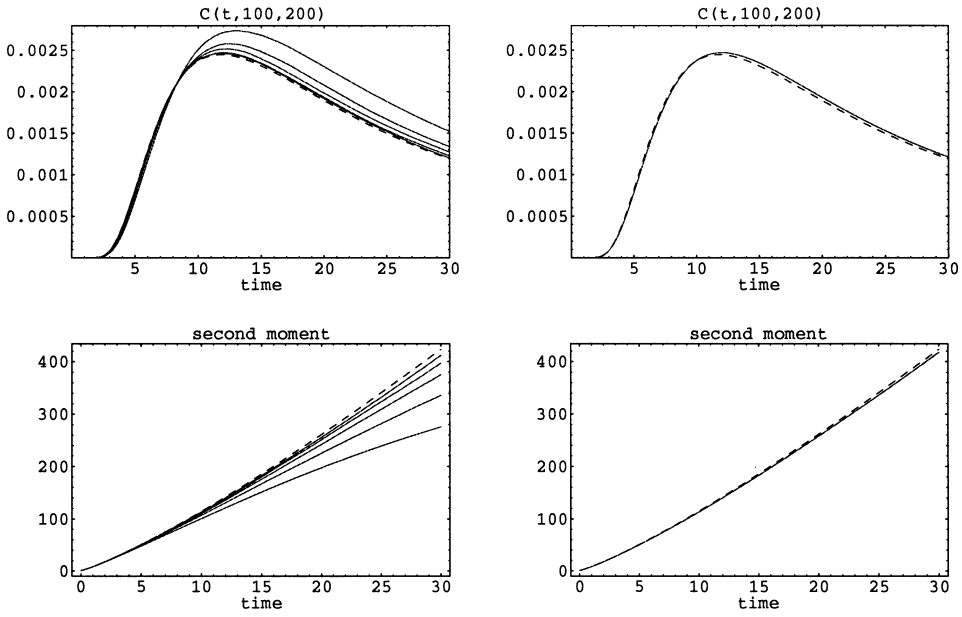

FIG. 1. *Approximation of functionals* (5.2), (5.3) *for kernel* (6.2) *using DSA* (*left*) *and MFA* (*right*).

of MFA started with N initial monomers is comparable to the systematic error of DSA started with $\tilde{N}/m_0(t)$ initial monomers. We consider a representation for the systematic error of the form

$$e^N_{sys}(t) \sim \frac{c(t)}{N}, \qquad \tilde{e}^{\tilde{N}}_{sys}(t) \sim \frac{\tilde{c}(t)}{\tilde{N}\, m_0(t)}. \tag{6.12}$$

The quotient

$$\frac{\tilde{c}(t)}{c(t)} \sim \frac{\tilde{e}^{\tilde{N}}_{sys}(t)\, \tilde{N}\, m_0(t)}{e^N_{sys}(t)\, N}, \tag{6.13}$$

obtained using data from Figure 2, is shown in Figure 3. Since this quantity is roughly constant, we obtain the following conclusions for the particular case under consideration. Both algorithms have the same order of convergence with respect to N. The time dependent constant for DSA carries an additional factor $m_0(t)^{-1}$. However, even taking into account the decreasing number of particles for DSA, there is still a factor of about six in favor of MFA.

6.2. *Systematic error and convergence in the gelling case.* Here we apply the algorithms to study the gelation phenomenon. The question arises how to approximate the gelation time (6.3) and, moreover, the *mass of the gel*

$$g(t) = m_1(0) - m_1(t), \qquad t \geq 0.$$

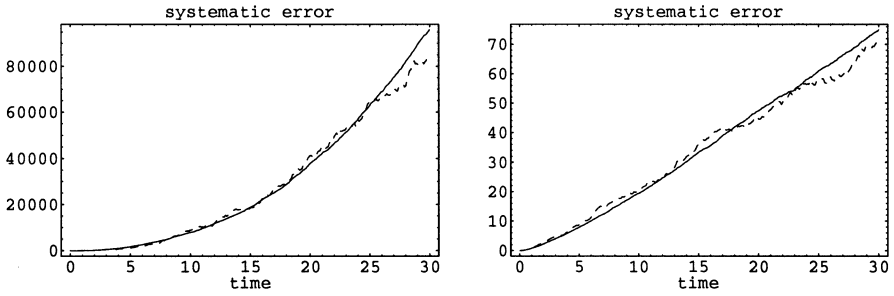

FIG. 2. *Normalized systematic error for* $m_2(t)$ *and kernel* (6.2) *using DSA* (*left*) *and MFA* (*right*).

Since the mass flow algorithm is not mass conserving, a straightforward approximation is [cf. (5.1)]

$$g^N(t) = m_1(0) - \frac{n(t)}{N}. \tag{6.14}$$

It is not so obvious how to determine the mass of the gel using the direct simulation algorithm. In [7] the truncation function $\Phi(N) = 0.5\,N$ is used to analyze the emergence of a "superparticle" having mass proportional to the mass of the system (cf. [5] and [20], Theorem 5 concerning more general truncation functions Φ). The emergence of a "superparticle" is closely related to one of Spouge's conjectures [31]: for the product kernel (6.4) the size $M_1(t)$ of the maximal cluster is of order N after the gelation time, and the gel mass can be identified with the maximal cluster, that is,

$$\tilde{g}^N(t) = \frac{M_1(t)}{N}. \tag{6.15}$$

This property is known for the multiplicative kernel (6.7) from random graph theory (cf. [2], Section 4.4. and citations therein).

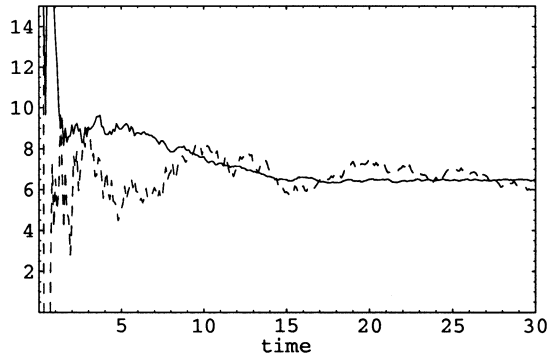

FIG. 3. *Quotient* (6.13) *of normalized systematic errors for* $m_2(t)$ *and kernel* (6.2).

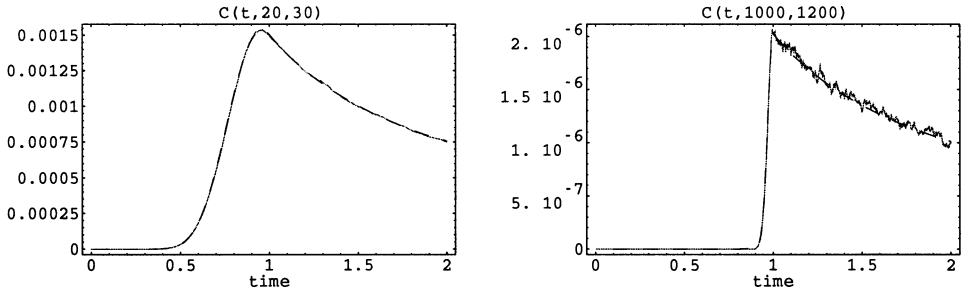

FIG. 4. *Approximation of sum concentrations of kernel* (6.7) *using MFA.*

First we consider the multiplicative kernel (6.7) so that analytical solutions are available. Figure 4 shows numerical approximations for various functionals of the form (5.2) using MFA with $N = b_N = 10^5$. The dashed lines correspond to the exact solutions (6.8). Though Theorem 3.2 does not cover this case, the numerical results show convergence of MFA to the unique solution. As mentioned above, DSA converges to the different limit (6.10). Figure 5 shows results concerning the approximation of the gel mass. The curves correspond to (6.14) for MFA with $N = b_N = 10^5$ (lower curve) and (6.15) for DSA with $N = 10^7$. These simulation results coincide with the exact curves (dashed) for the gel mass [cf. (6.9), (6.11)]. This observation strongly supports the conjecture that the MFA approximation (6.14) converges to the correct gel mass.

Next we consider the kernel (6.6), which reduces to the multiplicative kernel (6.7) for $\gamma = 2$. It is of interest to check which qualitative properties of the solutions are independent of γ. To get some impression, we consider the case $\gamma = 1.5$. Figure 6 shows results concerning the approximation of the gel mass. The curves correspond to (6.14) for MFA (lower curve) and (6.15) for DSA. The simulation results for different particle numbers (MFA: $N = 10^4, 10^5, b_N =$

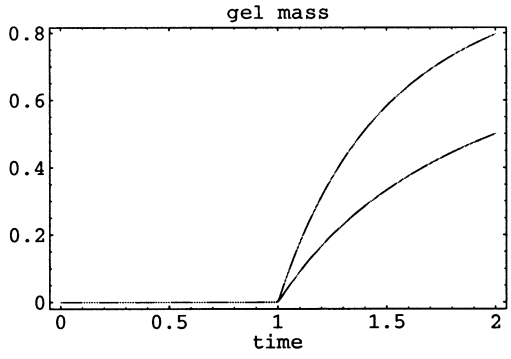

FIG. 5. *Approximations of gel mass for kernel* (6.7).

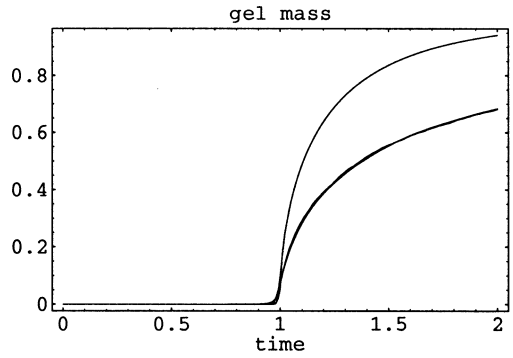

FIG. 6. *Approximations of gel mass for kernel* (6.6) *with* $\gamma = 1.5$.

10^5, DSA: $N = 10^7, 10^8$) coincide. Again we observe convergence of DSA and MFA to different solutions.

Finally we consider the product kernel (6.4) with $\alpha = 0.8$. Results concerning the approximation of the gel mass are displayed in Figure 7. The curves on the right plot correspond to (6.14) for MFA with initial monomer number $N = 10^2, 10^3, 10^4, 10^5$ and $b_N = 100\,N$. The results for $N = 10^4$ and $N = 10^5$ almost coincide indicating convergence of MFA. The conjecture that the limit is the mass of the gel is supported by the case of the multiplicative kernel considered above. The curves on the left plot correspond to (6.15) for DSA performed with $N = 10^5, \ldots, 10^9$ (solid lines from above to below). The dashed line indicates the result obtained from MFA with $N = 10^5$.

Note that DSA does not converge numerically, even for extremely large initial numbers of particles. This behavior is qualitatively different compared to results from Figures 5, 6. If the size of the maximal cluster was of smaller order than N then the curves would vanish in the limit $N \to \infty$. If Spouge's conjecture [cf. (6.15)] is correct, then the curves will come close to the dotted line. Moreover, there is the possibility that the curves stabilize between the

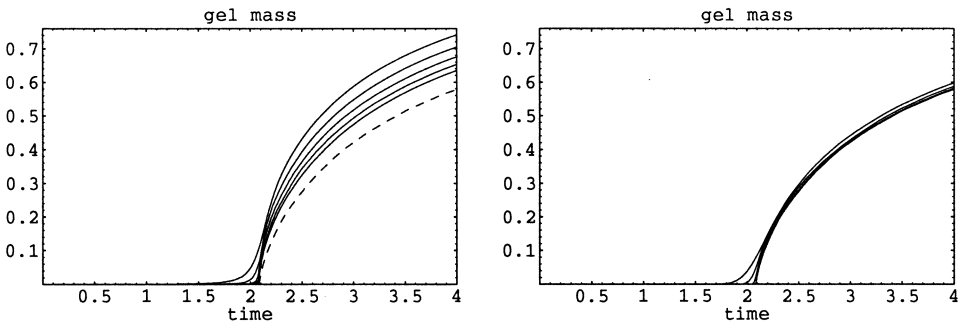

FIG. 7. *Approximations of gel mass for kernel* (6.4) *with* $\alpha = 0.8$.

time coordinate and the dotted line. Unfortunately, the true behavior cannot be concluded from these numerical results.

The poor convergence properties of DSA observed above have strong impact on the systematic error, even when calculating sum functionals (5.2). The convergence behavior of both algorithms for the functionals $C(t, 20, 30)$ (upper plots) and $C(t, 1000, 1200)$ (lower plots) is illustrated in Figure 8. The left plots show the DSA results. The solid lines belong to the simulations according to $N = 10^5, \ldots, 10^9$, from below to above. The dashed line represents the results for MFA with $N = 10^5$. The MFA results (right plots) for $N = 10^3, 10^4, 10^5$ and $b_N = 10^6$ almost coincide so that convergence is expected.

Again, convergence for DSA cannot be seen from these results (even for $N = 10^9$). Thus in the post-gelation phase the effect with the systematic error discussed in the previous subsection intensifies. Note that the number of particles for DSA at time $t = 4$ is still 15% of the initial number. However, in the case considered here one would expect convergence to the same limit (provided uniqueness of the solution). Slow convergence of DSA may be considered as a tendency, which becomes predominant in the limiting case $i\ j$, where both algorithms converge to different solutions.

6.3. *Statistical error and effort.* Here we discuss the issue of comparing the two algorithms regarding their efficiency. For many functionals, the mass flow algorithm provides estimators with lower variance compared to the direct

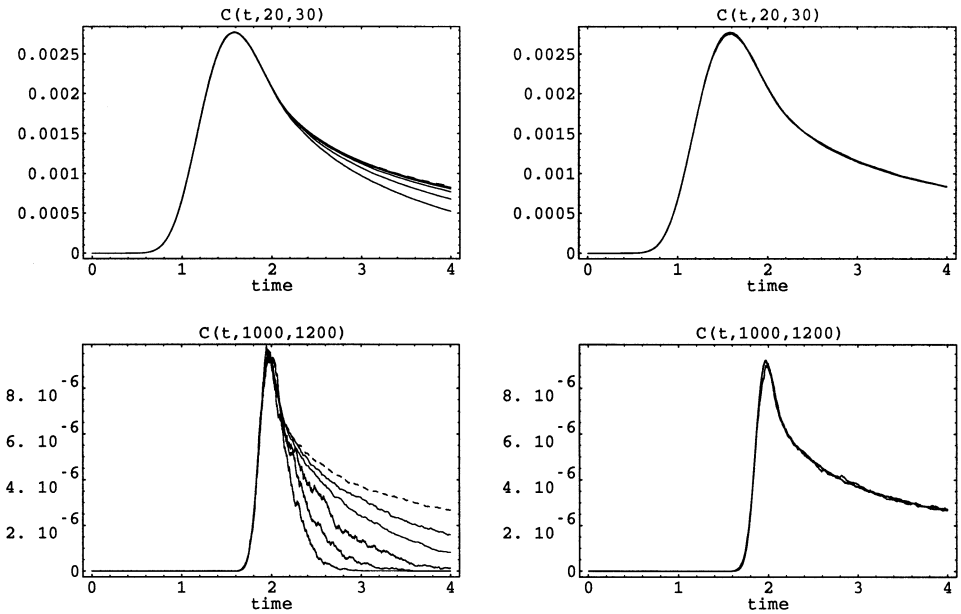

FIG. 8. *Approximation of sum concentrations for kernel* (6.4) *with* $\alpha = 0.8$ *using DSA* (*left*) *and MFA* (*right*).

simulation algorithm. This leads to a considerable gain in efficiency. The variance reduction is due to the fact that large particle sizes are resolved much more accurately.

Figure 9 gives an illustration of the described effect. Various bounded functionals of the form (5.2) are calculated for the product kernel (6.4) with $\alpha = 0.8$. The results in form of confidence bands are shown for DSA with $N = 10^7$ (left column) and for MFA with $N = b_N = 10^5$ (right column). The number of repetitions is $R = 10$ for DSA and $R = 30$ for MFA leading to approximately the same computation time. The systematic error is sufficiently small for both algorithms in the pre-gelation phase (cf. Figures 7, 8). The reference solution (dashed line) has been obtained from DSA with $N = 10^9$.

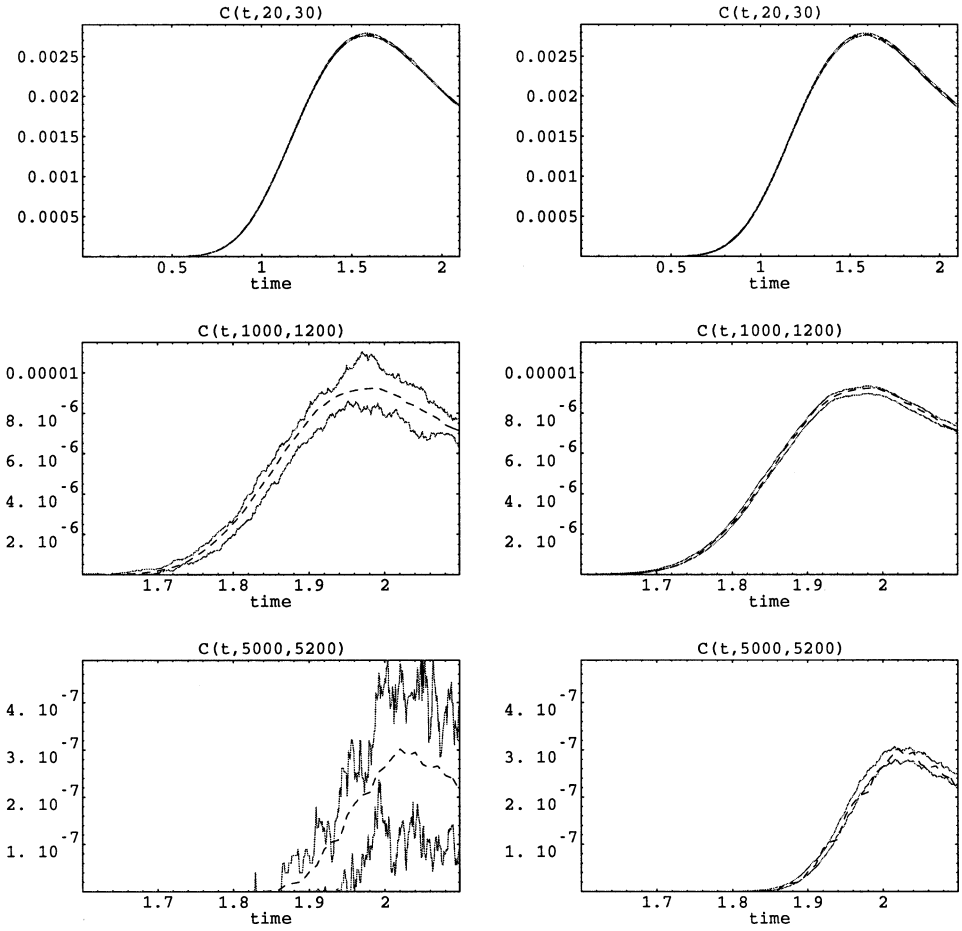

FIG. 9. *Confidence intervals for sum concentrations and kernel* (6.4) *with* $\alpha = 0.8$ *using DSA* (*left*) *and MFA* (*right*).

We will now study the structure of the gain factor (5.7) in more detail, in order to get a better understanding of the various quantities influencing efficiency. The variances Var $\tilde{\xi}^N(t)$, Var $\xi^N(t)$ and the values $\tilde{r}^N$, r^N (mean effort per trajectory) are asymptotically proportional to N^{-1} and N, respectively. Thus, it makes sense to define the derived quantities

$$\lim_{N\to\infty} N \text{ Var } \tilde{\xi}^N(t) = \tilde{C}_{\text{var}}(t), \qquad \lim_{N\to\infty} N \text{ Var } \xi^N(t) = C_{\text{var}}(t)$$

and

$$\lim_{N\to\infty} \frac{\tilde{r}^N(t)}{N} = \tilde{C}_{\text{eff}}(t), \qquad \lim_{N\to\infty} \frac{r^N(t)}{N} = C_{\text{eff}}(t).$$

The gain factor (5.7) is then approximated (as $\tilde{N}, N \to \infty$) in the form

$$\kappa(t) \sim \frac{\tilde{C}_{\text{eff}}(t)}{C_{\text{eff}}(t)} \frac{\tilde{C}_{\text{var}}(t)}{C_{\text{var}}(t)} =: \kappa_{\text{eff}}(t)\, \kappa_{\text{var}}(t).$$

Thus the relationship of the mean effort per trajectory and of the variances of the two estimators can be studied separately.

Note that the coefficient $\kappa_{\text{eff}}(t)$, representing the relationship of the effort, does not depend on the functional to be calculated. Figure 10 shows $\kappa_{\text{eff}}(t)$ for the kernel (6.2), indicating a considerable advantage of DSA on longer time intervals. This is not surprising since the number of particles in DSA permanently decreases, which makes this algorithm much faster.

Next we consider the coefficient $\kappa_{\text{var}}(t)$, representing relationship of the variances. Note that this quantity depends on the functional to be evaluated.

Figure 11 shows variance gain of MFA for different concentration functionals $c(t, k)$ and kernel (6.2) at time $t = 30$. The fluctuations are due to the fact that empirical estimates of the variances are used. A mean square fit (solid

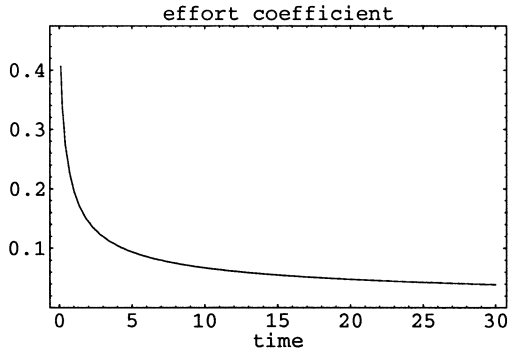

FIG. 10. *Effort coefficient* $\kappa_{\text{eff}}(t)$ *for the kernel* (6.2).

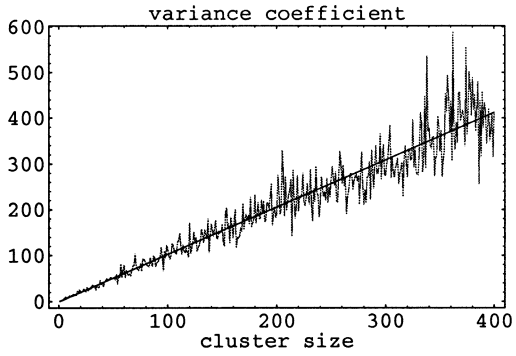

FIG. 11. *Variance coefficient* $\kappa_{\mathrm{var}}(t, k)$ *for concentration functionals and kernel* (6.2) *at* $t = 30$.

line) suggests the approximation

$$\kappa_{\mathrm{var}}(t, k) \sim k. \tag{6.16}$$

The property (6.16) has been observed for the different kernels at any fixed time $t < t_g$. Thus, one obtains

$$\kappa(t, k) \sim k\, \kappa_{\mathrm{eff}}(t),$$

which means that MFA resolves the cluster of size $k > \kappa_{\mathrm{eff}}(t)^{-1}$ more efficient than DSA.

Figure 12 shows the variance coefficient $\kappa_{\mathrm{var}}(t)$ and the efficiency gain factor $\kappa(t)$ for the second moment $m_2(t)$ and kernel (6.2). These curves show that MFA resolves the second moment more efficient than DSA, with the gain factor growing in time. Note that for the constant kernel a similar qualitative behavior is observed. In particular, a gain factors 20 is reached on the time interval $[0, 200]$.

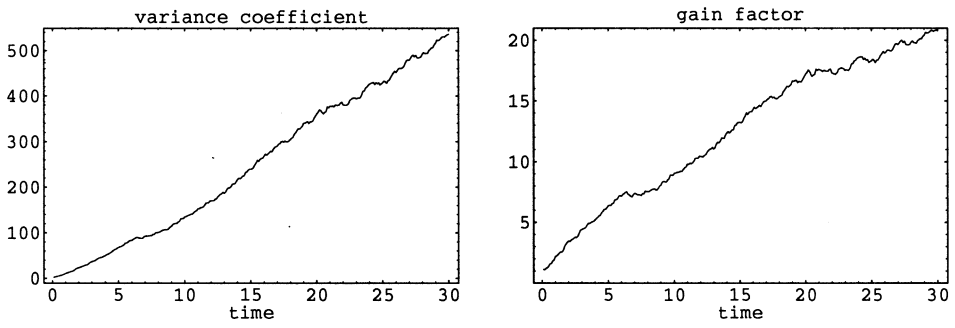

FIG. 12. *Variance coefficient* $\kappa_{\mathrm{var}}(t)$ *and efficiency gain factor* $\kappa(t)$ *for the second moment and kernel* (6.2).

7. Concluding remarks. A new Markov jump process approximating solutions of the coagulation equations (1.1), (1.2) has been introduced. Convergence results for the stochastic particle system were established, using techniques that had been successfully applied to the Marcus-Lushnikov process before. A stochastic numerical algorithm based on the new process has been described, and detailed numerical tests of this algorithm were presented. The numerical experiments illustrate the theoretical results, but also provide some insight into situations that have not yet been covered by the theory. This provides several suggestions and serves as a motivation for further theoretical investigations.

Our basic goal was the development of a stochastic algorithm for the numerical treatment of the coagulation equation, which has lower statistical fluctuations than the standard direct simulation algorithm (variance reduction). As the numerical tests show, this has been achieved to a considerable extent. Even when taking into account the effort needed to generate trajectories of the new process, the gain in efficiency is remarkable. However, the construction of a single algorithm and its successful testing in a number of examples can only be considered as a first step towards a general theory of variance reducing algorithms for the coagulation equation. It seems to be clear that, following the ideas of this paper, a whole class of algorithms can be constructed, where the single interaction between numerical particles consists in a transfer of appropriately chosen weights (instead of handling an interaction by imitating the physical process).

The new algorithm was constructed using an auxiliary equation for the mass flow of the coagulating system. This led to the conservation of the number of numerical particles (corresponding to mass conservation in the direct simulation) before the gelation point. This feature is very convenient from a computational point of view. Note that in the direct simulation approach several modifications have been introduced in order to keep the number of simulation particles sufficiently large. These modifications, which also produce a variance reducing effect, have not yet been compared to the mass flow algorithm.

One of the interesting features of the new algorithm is the much better convergence behavior (compared to the direct simulation algorithm) after the gelation point for kernels of the form (6.4). This seems to be due to the fact that there is no gel-sol interaction in the mass flow algorithm, while there is such an interaction in the direct simulation algorithm. For kernels (6.4) this interaction is not strong enough to be kept in the limit, but it causes additional systematic error for finite particle systems. On the other hand, for kernels of the form (6.6) the gel-sol interaction is so strong that both algorithms converge to different limits. However, a reasonable conjecture based on the numerical observations is that the mass loss detected by the mass flow algorithm converges to the correct mass of the gel in Smoluchowski's coagulation equation. A further interesting feature of the mass flow process is that it seems to show explosion at the gelation point (if the truncation parameter

tends to infinity). This would connect the gelation phenomenon (a property of the limiting equation) with the explosion time of a stochastic process.

Acknowledgments. The authors appreciate useful discussions with H. Babovsky on the results contained in [3], and with K. Sabelfeld on numerical issues related to the coagulation equation.

REFERENCES

[1] ALDOUS, D. (1998). Emergence of the giant component in special Marcus-Lushnikov processes. *Random Structures Algorithms* **12** 179–196.
[2] ALDOUS, D. (1999). Deterministic and stochastic models for coalescence (aggregation and coagulation): a review of the mean-field theory for probabilists. *Bernoulli* **5** 3–48.
[3] BABOVSKY, H. (1999). On a Monte Carlo scheme for Smoluchowski's coagulation equation. *Monte Carlo Methods Appl.* **5** 1–18.
[4] BAUER, H. (1990). *Maß- und Integrationstheorie*. de Gruyter, Berlin.
[5] BUFFET, E. and PULE, J. V. (1990). On Lushnikov's model of gelation. *J. Statist. Phys.* **58** 1041–1058.
[6] BUFFET, E. and PULE, J. V. (1991). Polymers and random graphs. *J. Statist. Phys.* **64** 87–110.
[7] DOMIOVSKII, E. R., LUSHNIKOV, A. A. and PISKUNOV, V. N. (1978). Monte Carlo simulation of coagulation processes. *Dokl. Akad. Nauk SSSR Ser. Phys. Chem.* **240** 108–110. In Russian.
[8] DRAKE, R. L. (1972). A general mathematical survey of the coagulation equation. In *Topics in Current Aerosol Research (Part 2)* (G.M. Hidy and J.R. Brock, eds) 201–376. Pergamon Press, Oxford.
[9] EIBECK, A. and WAGNER, W. (2000). An efficient stochastic algorithm for studying coagulation dynamics and gelation phenomena. *SIAM J. Sci. Comput.* **22** 802–821.
[10] EIBECK, A. and WAGNER, W. (2000). Approximative solution of the coagulation-fragmentation equation by stochastic particle systems. *Stochastic Anal. Appl.* **18** 921–948.
[11] ETHIER, S. N. and KURTZ, T. G. (1986). *Markov Processes, Characterization and Convergence*. Wiley, New York.
[12] FISHMAN, G. S. (1996). *Monte Carlo: Concepts, Algorithms, and Applications*. Springer, New York.
[13] GARCIA, A. J., VAN DEN BROECK, C., AERTSENS, M. and SERNEELS, R. (1987). A Monte Carlo simulation of coagulation. *Phys. A* **143** 535–546.
[14] GILLESPIE, D. N. (1972). The stochastic coalescence model for cloud droplet growth. *J. Atmospheric Sci.* **29** 1496–1510.
[15] GILLESPIE, D. N. (1975). An exact method for numerically simulating the stochastic coalescence process in a cloud. *J. Atmospheric Sci.* **32** 1977–1989.
[16] GUERON, S. (1998). The steady-state distributions of coagulation-fragmentation processes. *J. Math. Biol.* **37** 1–27.
[17] GUIAŞ, F. (1997). A Monte Carlo approach to the Smoluchowski equations. *Monte Carlo Methods Appl.* **3** 313–326.
[18] GUIAŞ, F. (1999). A direct simulation method for the coagulation-fragmentation equations with multiplicative coagulation kernels. *Monte Carlo Methods Appl.* **5** 283–309
[19] HEILMANN, O. J. (1992). Analytical solutions of Smoluchowski's coagulation equation. *J. Phys. A* **25** 3763–3771.
[20] JEON, I. (1998). Existence of gelling solutions for coagulation-fragmentation equations. *Comm. Math. Phys.* **194** 541–567.
[21] KOLODKO, A., SABELFELD, K. and WAGNER, W. (1999). A stochastic method for solving Smoluchowski's coagulation equation. *Math. Comput. Simulation* **49** 57–79.
[22] KOLODKO, A. A. and WAGNER, W. (1997). Convergence of a Nanbu type method for the Smoluchowski equation. *Monte Carlo Methods Appl.* **3** 255–273.

[23] KOUTZENOGII, K. P., LEVYKIN, A. I. and SABELFELD, K. K. (1996). Numerical simulation of the kinetics of aerosol formation in the free molecular collision regime. *J. Aerosol Sci.* **27** 665–679.
[24] LIFFMAN, K. (1992). A direct simulation Monte Carlo method for cluster coagulation. *J. Comput. Phys.* **100** 116–127.
[25] LUSHNIKOV, A. A. (1978). Some new aspects of coagulation theory. *Izv. Akad. Nauk SSSR Ser. Fiz. Atmosfer. i Okeana* **14** 738–743.
[26] MARCUS, A. H. (1968). Stochastic coalescence. *Technometrics* **10** 133–148.
[27] NORRIS, J. R. (1999). Smoluchowski's coagulation equation: uniqueness, nonuniqueness and a hydrodynamic limit for the stochastic coalescent. *Ann. Appl. Probab.* **9** 78–109.
[28] SABELFELD, K. K. (1998). Stochastic models for coagulation of aerosol particles in intermittent turbulent flows. *Math. Comput. Simulation* **47** 85–101.
[29] SABELFELD, K. K. and KOLODKO, A. A. (1997) Monte Carlo simulation of the coagulation processes governed by Smoluchowski equation with random coefficients. *Monte Carlo Methods Appl.* **3** 275–311.
[30] SABELFELD, K. K., ROGAZINSKII, S. V., KOLODKO, A. A. and LEVYKIN, A. I. (1996). Stochastic algorithms for solving Smoluchowski coagulation equation and applications to aerosol growth simulation. *Monte Carlo Methods Appl.* **2** 41–87.
[31] SPOUGE, J. L. (1985). Monte Carlo results for random coagulation. *J. Colloid Interface Sci.* **107** 38–43.
[32] VON SMOLUCHOWSKI, M. (1916). Drei Vorträge über Diffusion, Brownsche Molekularbewegung und Koagulation von Kolloidteilchen. *Phys. Z.* **17** 557–571, 585–599.

WEIERSTRASS INSTITUTE FOR APPLIED ANALYSIS
AND STOCHASTICS
MOHRENSTRAßE 39
D–10117 BERLIN
GERMANY
E-MAIL: eibeck@wias-berlin.de
wagner@wias-berlin.de